# Observation of New Rydberg Series and Resonances in Doubly Excited Helium at Ultrahigh Resolution

K. Schulz, G. Kaindl, and M. Domke
*Institut für Experimentalphysik, Freie Universität Berlin, Arnimallee 14, D-14195 Berlin-Dahlem, Germany*

J. D. Bozek, P. A. Heimann, and A. S. Schlachter
*Advanced Light Source, Lawrence Berkeley National Laboratory, 1 Cyclotron Road, Berkeley, California 94720*

J. M. Rost
*Fakultät für Physik, Universität Freiburg, Hermann-Herder-Strasse 3, D-79104 Freiburg, Germany*
(Received 18 April 1996; revised manuscript received 31 July 1996)

We report on a striking improvement in spectral resolution in the soft x-ray range to 1.0 meV at 64.1 eV, measured via the $\mu$eV-wide $2,-1_3$ double-excitation resonance of helium. This ultrahigh resolution combined with the high photon flux at undulator beam line 9.0.1 of the Advanced Light Source have allowed observation of new Rydberg series and resonances below the $N = 3$ threshold of doubly excited He. The obtained resonance parameters (energies, lifetime widths, and Fano-$q$ parameters) are in excellent agreement with the results of state-of-the-art calculations. [S0031-9007(96)01322-1]

PACS numbers: 32.80.Fb, 31.50.+w, 32.70.Jz

Doubly excited helium is the prototypical neutral system for the study of electron-electron correlations. Since the pioneering work of Madden and Codling [1] and its interpretation by Cooper *et al.* [2], a number of experimental [3–6] and theoretical [6–14] studies of the $^1P^o$ double-excitation states of He have been performed. Despite these efforts, only few of the optically allowed Rdyberg series could be observed up to now, mainly due to small excitation cross sections. Nevertheless, all three $^1P^o$ Rydberg series below the $N = 2$ threshold $I_2$ [5], two out of five series below the $N = 3$ threshold $I_3$ [4], and the strongest resonance of a third $N = 3$ series [6] have previously been identified.

The present Letter reports on striking progress in energy resolution in the energy range of grazing-incidence grating monochromators and its application to previously unobservable states of doubly excited He. By monitoring an extremely narrow double-excitation resonance of He with a theoretical lifetime width of $\leq 5$ $\mu$eV [6], a resolution of $\Delta E = 1.0$ meV (FWHM) at 64.1 eV has been achieved. This unprecedented spectral resolution, combined with high photon flux, allowed the investigation of new Rydberg resonances below $I_3$, including a detailed comparison with *ab initio* calculations.

The experiments were performed at undulator beam line 9.0.1 of the Advanced Light Source (ALS), which is equipped with a spherical-grating monochromator (the 925-lines/mm grating was used here) [15]. Energy was calibrated by fitting the principal series below $I_2$ and $I_3$ to Rydberg series of Fano profiles and adjusting the energy-defining monochromator parameters to match the correct threshold energies, $I_2 = 65.4007$ eV and $I_3 = 72.9589$ eV; the latter were obtained by adding the first ionization potential of He, $I_1 = 24.5874$ eV, to the He II spectrum. The uncertainty in energy calibration (Gaussian $\sigma$) was estimated as 1.7 meV below $I_2$ and 1.0 meV between $I_2$ and $I_3$. For comparison with theoretical values in atomic units, a Rydberg constant $R = 13.603\,83$ eV and a double-ionization potential $I_\infty = 79.0052$ eV were used. Measurements were performed with a gas cell containing two parallel charge-collecting plates of 10-cm active length, filled with He at pressures from 2 to 500 $\mu$bar, and separated from the monochromator by a window of 1500 Å Al(1%Si) (1200 Å carbon) for $h\nu < I_2$ ($h\nu > I_2$). All spectra were normalized to the incident photon flux monitored with a gold grid in front of the gas cell. The electric currents in the gas cell and on the gold grid ($10^{-11}$ to $10^{-10}$ A) were measured with sensitive current amplifiers (Keithley model 428).

The photoionization spectrum below $I_2$ is shown in Fig. 1, where the states are denoted by $N, K_n$; $N$ and $n$ (or $n', n''$) refer to the principal quantum numbers of the inner and outer electrons, respectively, and $K$ to a correlation quantum number (see below). The principal series $2,0_n$, shown in (a) for $n \geq 4$, was resolved up to $n = 26$ [see inset in 1(a)]. The stronger secondary series $2,1_{n'}$, shown on an expanded energy scale in 1(b) and 1(c), was observed up to $n' = 12$, and the weaker secondary series $2,-1_{n''}$, up to $n'' = 7$. While most spectra were recorded with 5-$\mu$m-wide entrance and exit slits, corresponding to $\Delta E \cong 2$ meV, the $2,1_4$ and $2,-1_3$ resonances were measured with 2.5-$\mu$m-wide slits at highest resolution. The $2,-1_3$ state is ideally suited for determining monochromator resolution due to its narrow width, calculated as $\leq 5$ $\mu$eV [5,6]. The inset in 1(b) shows this resonance on an expanded energy scale, with a total width

 0031-9007/96/77(15)/3086(4)$10.00 

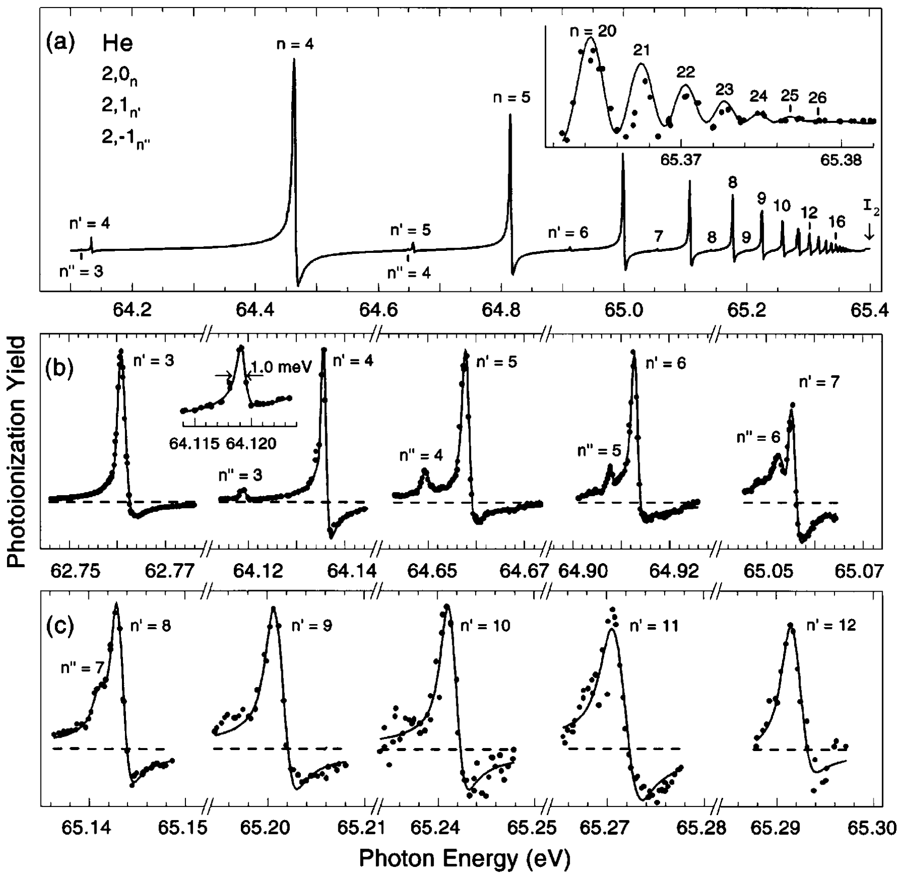


FIG. 1. Autoionizing resonances of doubly excited He below $I_2$: (a) overview spectrum, with resonances of all three ${}^1P^o$ Rydberg series; (b),(c) resonances of the secondary series $2,1_{n'}$ and $2,-1_{n''}$. Smooth backgrounds, caused by neighboring principal resonances, have been subtracted from the data.

of 1.0 meV (FWHM), corresponding to a resolving power of $E/\Delta E = 64\,000$ at 64.1 eV, i.e., by a factor of 4 better than previously obtained with the SX700/II monochromator at BESSY [5]. The photon flux at this ultrahigh resolution was measured with a Si photodiode to be $\cong 8 \times 10^9$ photons/s at $h\nu = 62$ eV (300 mA ring current; 2.5 $\mu$m slits), about a factor of 40 higher than at the SX700/II beam line at $\Delta E = 4$ meV.

The classification scheme for doubly excited states in He used here has been introduced by Herrick and Sinanoğlu [7] and Lin [8]. The states are denoted by $N(K,T)_n^{A\ 2S+1}L^{\pi}$, where $L$, $S$, and $\pi$ have their usual meaning and $K$, $T$, and $A$ are correlation quantum numbers. $K$ ranges from $N-T-1$, $N-T-3, \ldots, -(N-T-1)$, and $T$ can be 0 or 1 for ${}^1P^o$ states. Both $K$ and $T$ describe the angular correlation between the two electrons, while $A$ measures the radial correlation [8]. Photoexcitation from the $1(0,0)_1^{+\ 1}S^e$ ground state leads to ${}^1P^o$ states, and $(2N-1)\,{}^1P^o$ Rydberg series exist for each $N$. We use here the abbreviated classification $N,K_n$ as introduced by Zubek *et al.* [3]. There are three ${}^1P^o$ series converging to $I_2$: $2,\ 0_n$ with $T=1$ and $A=+1, 2, 1_{n'}$ with $T=0$ and $A=-1$, and $2,-1_{n''}$ with $T=0$ and $A=0$. Originally, these three series had been denoted by $(sp, 2n+)$, $(sp, 2n-)$, and $(2p, nd)$, respectively [1]. Five ${}^1P^o$ series converge to $I_3$: $3,1_n$ and $3,-1_n$ with $T=1$ and $A=+1$; $3,2_n$ and $3,0_n$ with $T=0$ and $A=-1$; and $3,-2_n$ with $T=0$ and $A=0$.

The spectra in Fig. 1 were least-squares fitted with independent Fano profiles convoluted with the monochromator function, which deviates slightly from a pure Gaussian and could be adequately described by Hermitian polynomials up to fourth order multiplied by a Gaussian; the solid lines through the data points represent the fit results. The principal resonances $2,0_n$ were measured with a relatively low He pressure (2 $\mu$bar) to exclude saturation effects, which had been seen in earlier measurements [6]. The derived resonance energies $E_r$, lifetimes widths $\Gamma$, and Fano-$q$ parameters, listed in Table I(a), are of considerably improved accuracy due to the high energy resolution and the low He pressure. The resonances of the $2,-1_{n''}$ series were found to be too narrow to allow fits with Fano profiles, with the exception of the $2,-1_3$ resonance, for which $\Gamma < 10$ $\mu$eV and $q < -2$ were obtained. The energy differences $\delta E$ between the $2,-1_{n''}$ and the nearby $2,1_{n'}$ resonances are $-16.5(5)$ meV $[2,-1_3/2,1_4]$, $-8.7(5)$ meV $[2,-1_4/2,1_5]$, $-5.0(5)$ meV $[2,-1_5/2,1_6]$, $-3.4(5)$ meV $[2,-1_6/2,1_7]$, and $-1.9(5)$ meV $[2,-1_7/2,1_8]$.

A comparison of the present experiment with all

TABLE I. Summary of derived resonance parameters below (a) $I_2$ and (b) $I_3$: Energy $E_r$, linewidth $\Gamma$, and Fano-$q$ parameter, in comparison with theoretical results by Wintgen and Delande [11] and Sánchez and Martín [12]. The numbers in parentheses represent the error bars in units of the last digit.

| | This work | | | Wintgen and Delande | | | Sánchez and Martín | | |
|---|---|---|---|---|---|---|---|---|---|
| Resonance | $E_r$ (eV) | $\Gamma$ (meV) | $q$ | $E_r$ (eV) | $\Gamma$ (meV) | $q$ | $E_r$ (eV) | $\Gamma$ (meV) | $q$ |
| (a) $N = 2$ $2,0_2$ | 60.1503(40) | 37.6(2) | −2.73(4) | 60.1466 | 37.36 | −2.77 | 60.156 | 38.3 | −2.83 |
| $2,0_3$ | 63.6575(30) | 8.3(5) | −2.53(4) | 63.6578 | 8.19 | −2.58 | 63.661 | 8.39 | −2.67 |
| $2,0_4$ | 64.4655(20) | 3.4(7) | −2.58(5) | 64.4664 | 3.49 | −2.55 | 64.467 | 3.58 | −2.64 |
| $2,1_3$ | 62.7610(20) | 0.11(2) | −4.1(4) | 62.7602 | 0.105 | −4.25 | 62.760 | 0.112 | −3.75 |
| $2,1_4$ | 64.1358(20) | 0.06(2) | −2.4(5) | 64.1364 | 0.055 | −3.32 | 64.137 | 0.057 | −2.93 |
| $2,1_5$ | 64.6586(20) | 0.03(3) | −2.8(5) | 64.6587 | 0.027 | −3.31 | 64.659 | 0.028 | −2.89 |
| (b) $N = 3$ $3,2_4$ | 71.2254(14) | 1.0(5) | 2.3(10) | 71.2251 | 0.928 | 3.33 | 71.2252 | 0.833 | −17.85 |
| $3,2_5$ | 72.0027(14) | 0.6(4) | 3.1(10) | 72.0011 | 0.599 | 4.52 | 72.0011 | 0.548 | −10.59 |
| $3,2_6$ | 72.3577(14) | 0.17(30) | 4.8(10) | 72.3553 | 0.357 | 5.74 | 72.3561 | 0.343 | −20.45 |
| $3,2_7$ | 72.5489(14) | 0.06(30) | 2.7(20) | 72.5451 | 0.221 | 7.35 | ... | ... | ... |
| $3,2_8$ | 72.6614(14) | <0.3 | >1 | 72.6582 | 0.144 | 8.68 | ... | ... | ... |
| $3,0_4$ | 71.7247(14) | 0.1(3) | 1.6(20) | 71.7232 | 0.615 | 0.44 | 71.7239 | 0.454 | 0.557 |
| $3,0_5$ | 72.2530(14) | 0.05(30) | 10(20) | 72.2516 | 0.288 | 0.77 | 72.2519 | 0.200 | 0.935 |

existing theoretical results would exceed the frame of this Letter. Therefore the results of only two theoretical approaches [11,12] have been included in Table I; they generally agree well with experiment, better than with previous experimental values [3–6].

With this substantial improvement in resolution and photon flux, we searched for previously unobservable double-excitation resonances. Figure 2(a) shows an overview spectrum below $I_3$, dominated by the principal series $3{,}1_n$ and the lowest resonance $3,-1_3$ of the strongest secondary series; the energies of the newly discovered resonances of the secondary series $3{,}2_n$ and $3{,}0_n$ (see below) have been marked by vertical arrows.

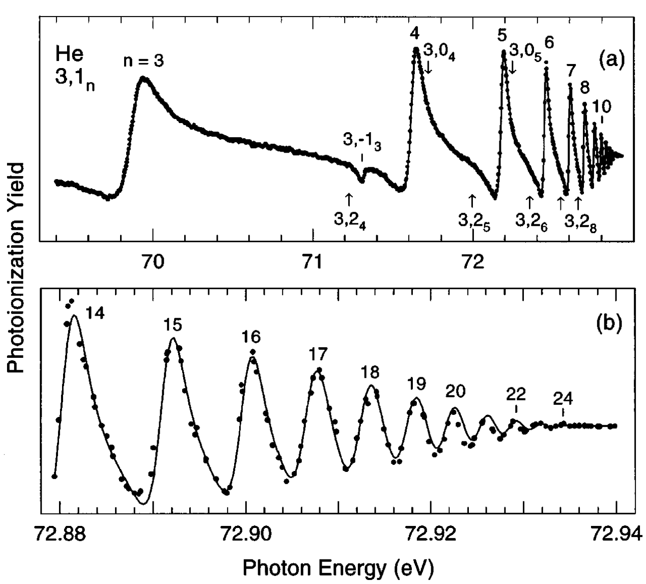


FIG. 2. Autoionizing resonances below $I_3$: (a) overview (from Ref. [6]); (b) upper region shown on an expanded energy scale (present work).

Figure 2(b) shows the principal series $3{,}1_n$ for $n \geq 14$ resolved up to $n = 24$ at $\Delta E \cong 2.3$ meV.

The $3{,}2_n$ and $3{,}0_n$ resonances are shown in Fig. 3; both series have $T = 0$ and $A = -1$ and are "quasiforbidden" [7,13]. A search for the extremely narrow lowest resonance of the fifth $N = 3$ series, $3,-2_n$ (with $T = 0$ and $A = 0$), with a strongly reduced excitation cross section [11], was unsuccessful. Hence all series with $T = 1$ or 0 and $A = +1$ or $-1$ below $I_2$ and $I_3$ have now been observed. The series with $T = 1$, $A = +1$ are the most intense ones, exhibiting also the largest lifetime widths. The series with $T = 0$, $A = -1$ are weaker and narrower, and the weakest and narrowest resonances have $A = 0$, which could be monitored for $N = 2$ only. Note that series with the same $T$ and $A$ get weaker for decreasing $K$.

These variations in intensity and linewidth reflect differences in the correlated electron motion in the various excited states, in agreement with the results of *ab initio* calculations [6,9–12]. Electron correlations can be described in a rather direct way by a "molecular" picture, where the electron-electron vector $\mathbf{r} = \mathbf{r}_1 - \mathbf{r}_2$ is taken as an adiabatic, approximate quantization axis. In this way, propensity rules for photoabsorption [13] and autoionization [14] have been derived, which predict that in photoabsorption transitions to states with $v_2 = 0$ or 1 are favored; here $v_2 = N - K - 1$ is a quantum number of the collective two-dimensional harmonic motion around the saddle point ($\mathbf{r}_1 = -\mathbf{r}_2$) of the two-electron potential. In autoionization, large (small) widths are predicted for $A = +1$ ($A = -1$), since the respective states have an antinode (node) on the saddle point, coupling stronger (weaker) to the continuum above $I_{N-1}$. These propensity rules are confirmed in the present experiment; a more detailed discussion will be given elsewhere [16].

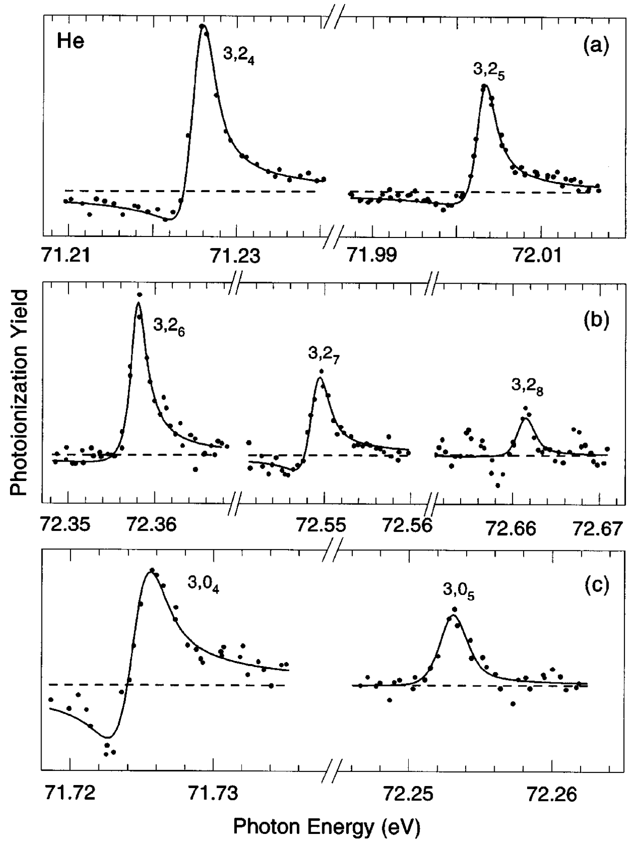


FIG. 3. Newly observed resonances of two secondary series below $I_3$: (a),(b) $3,2_n$ series up to $n = 8$; (c) $3,0_n$ series up to $n = 5$. Smooth backgrounds, caused by neighboring resonances, have been subtracted.

The parameters of the $3,2_n$ and $3,0_n$ resonances, derived by fit, are included in Table I(b), together with theoretical results [11,12]. While the energies are very accurate, $\Gamma$ and $q$ are subject to relatively large error bars, since the natural widths are much smaller than resolution, and saturation effects could not be excluded due to the rather high He pressure of 460 $\mu$bar required for reasonable signal-to-noise ratios. The experimental parameters are generally in good agreement with the results of state-of-the-art calculations, with the exception of the $q$ parameters of the $3,2_n$ series [12]; however, only few theories have calculated $q$ parameters until now.

The ultimate resolving power of beam line 9.0.1 is 178 000, given by the number of grooves in the 925 lines/mm grating. However, several factors degrade resolution, including the finite widths of the entrance and exit slits, the coma aberration, figure errors of the optical surfaces, and the finite mechanical stability. Even though the coma error is small at 64.1 eV (the Rowland-circle condition is fulfilled at $\cong 71$ eV with the grating used), the results reflect the extraordinary quality of the optical grating (with a figure error better than 0.5 $\mu$rad rms). Beam line 9.0.1 at the ALS is thus a powerful new tool for ultrahigh resolution spectroscopy of atoms, molecules, and condensed matter.

The authors acknowledge expert help by the operating staff of ALS as well as valuable discussions with H. Padmore, T. Warwick, D. DiGennaro, and W. McKinney. The work was supported by the Bundesminister für Bildung, Wissenschaft, Forschung und Technologie, Project No. 05-650-KEA, the Deutsche Forschungsgemeinschaft, Project No. Do 561/1-1, and the U.S. Department of Energy, Contract No. DE-AC03-76F00098.

[1] R. P. Madden and K. Codling, Phys. Rev. Lett. **10**, 516 (1963); Astrophys. J. **141**, 364 (1965).
[2] J. W. Cooper, U. Fano, and F. Prats, Phys. Rev. Lett. **10**, 518 (1963).
[3] M. Zubek *et al.*, J. Phys. B **22**, 3411 (1989).
[4] M. Domke *et al.*, Phys. Rev. Lett. **66**, 1306 (1991).
[5] M. Domke, G. Remmers, and G. Kaindl, Phys. Rev. Lett. **69**, 1171 (1992).
[6] M. Domke *et al.*, Phys. Rev. A **53**, 1424 (1996).
[7] D. R. Herrick and O. Sinanoğlu, Phys. Rev. A **11**, 97 (1975).
[8] C. D. Lin, Phys. Rev. A **29**, 1019 (1984).
[9] J.-Z. Tang, S. Watanabe, and M. Matsuzawa, Phys. Rev. A **48**, 841 (1993).
[10] T. N. Chang, Phys. Rev. A **47**, 3441 (1993).
[11] D. Wintgen and D. Delande, J. Phys. B **26**, L399 (1993); (private communication).
[12] I. Sánchez and F. Martín, J. Phys. B **23**, 4263 (1990); Phys. Rev. A **44**, 7318 (1991).
[13] A. Vollweiter, J. M. Rost, and J. S. Briggs, J. Phys. B **24**, L155 (1991).
[14] J. M. Rost and J. S. Briggs, J. Phys. B **23**, L339 (1990).
[15] P. A. Heimann *et al.*, Nucl. Instrum. Methods Phys. Res., Sect. A **319**, 106 (1992).
[16] J. M. Rost *et al.* (to be published).